Impact of Pipe Leakage Location on Siphon Flow Breakage

Sumit R. Zanje, S.M.ASCE¹; Vivek Verma, Ph.D.²; Linlong Bian, Ph.D.³; Zeda Yin⁴; and Arturo S. Leon, Ph.D., P.E., D.WRE⁵

¹Dept. of Civil and Environmental Engineering, Florida International Univ.

(corresponding author). Email: szanj001@fiu.edu

²Dept. of Civil and Environmental Engineering, Florida International Univ.

Email: vverm002@fiu.edu

³Dept. of Civil and Environmental Engineering, Florida International Univ.

Email: lbian003@fiu.edu

⁴Dept. of Civil and Environmental Engineering, Florida International Univ.

Email: zyin005@fiu.edu

⁵Dept. of Civil and Environmental Engineering, Florida International Univ.

Email: arleon@fiu.edu

ABSTRACT

Siphons are often used for releasing water by gravity, especially from shallow ponds. This paper investigates the hydrodynamic characteristics of the flow in a siphon under leakage (e.g., pipe puncture) and no-leakage conditions using the OpenFOAM Computational Fluid Dynamics (CFD) package. The volume-of-fluid (VOF) method was used to solve the air-water two-phase flow, and the standard k-\varepsilon model was used to model the turbulence. The CFD model was assessed using experimental measurements for the no-leakage condition. The simulations for the leakage condition focused on investigating the siphon flow break phenomenon as a function of leakage location. The results show the impact of leak position on the siphon flow break and the suitability of OpenFOAM for simulating the complex two-phase flow dynamics that occurs in a siphon.

Keywords: CFD, OpenFOAM, siphon leakage, volume-of-fluid (VOF), water storage management.

INTRODUCTION

A siphon essentially consists of an inverted 'U' pipe, one end of which is held in contact with the reservoir on the upstream side, and the downstream end of the siphon has an elevation lower than the reservoir water level (Qin et al. 2019; Leon and Verma 2019). Many researchers reviewed this phenomenon to understand its working mechanism (Hughes 2010; Ramette and Ramette 2011; Richert and Binder 2011). Hughes (2010) is notable for discovering a 99-year-old error in the Oxford dictionary and correcting the operating force of a siphon, which is gravity rather than atmospheric pressure. Babaeyan-Koopaei et al. (2002) provided a detailed explanation of siphon spillways operating stages. Kang et al. (2013) experimentally investigated the effect of the size and type of the siphon breaker, size and position of loss-of-coolant accident (LOCA), and the presence of an orifice on siphon performance. Cai et al. (2014) experimentally investigated flow pattern variables and relevant influencing factors at the top of siphon hoses on drainage flow. Despite its difficulty, the energy equation can explain the siphon flow well. Leon and Alnahit (2016) investigated the drainage of a tank using a siphon and found a good

agreement between measured data, the energy equation, and three-dimensional (3D) numerical simulations. Viridi et al. (2011) used the molecular dynamics (MD) method to investigate the maximum siphon height at which the siphon still can flow water. Aydin et al. (2015) investigated the hydrodynamic characteristics of siphon using volume-of-fluid (VOF) formulation. The study shows that pressure and velocity distribution inside the siphon and discharge performance agree with experimental and theoretical data (analytical and energy equation).

This paper investigates the hydrodynamic characteristics of a siphon and analyzes the siphon break phenomenon caused by a leakage in the siphon pipe and when the liquid falls below the pipe inlet elevation. This paper is divided as follows: First, the experimental work is briefly presented for the no-leakage condition. Second, a computational fluid dynamics model is developed using OpenFOAM and validated using the experimental data. Third, the validated CFD model is used to investigate the siphon break phenomenon associated with a leakage in the siphon pipe. Finally, key concluding remarks are made.

EXPERIMENTAL WORK

The apparatus for the experimental study is shown schematically in Figure 1. The siphon consisted of PVC pipe schedule 40 with an internal diameter (D) of 0.152 mm (6 in) and an actuated butterfly valve at the outlet. The total length of the siphon pipe is approximately 7.6 m (25 ft). The water tank has a maximum capacity of 9.463 m³ (2,500 gals) with a diameter of 2.286 m (90 in) and a height of 2.489 m (98 in). A check valve is used to prevent backward flow. A bilge pump is used for the siphon priming. An extended sight tube consisting of clear PVC schedule 40 with an internal diameter (D) of 0.152 mm (6 in) was used to visualize and control the priming. An air vent and two-level switches are connected to the sight tube to control the priming, as shown in Figure 2 (Verma et al. 2020a; Bian et al. 2021). The data collected in the experiments include water elevation in the tank (H) and flow discharge (Q). The water level in the tank was measured using the LVCN-414 level meter sensor. The flow discharge in the pipe was measured using an FDT-47 sensor with V mounting style. For more details on the experimental setup, the reader is referred to Verma et al. 2021 and Verma et al. 2020b.

Figure 3 shows a complete time trace for the water elevation in the tank (red line) and the flow discharge in the siphon (blue line) for the no-leakage condition. The jump around the 5^{th} second indicates the opening of the butterfly valve and the subsequent water release out of the tank. Similarly, a sudden drop at about 145^{th} second indicates that the butterfly valve is being closed. The maximum flow recorded by the instrument FDT-47 is about 40 L/s at around 25^{th} second, associated to a water depth of 1.94 m.

NUMERICAL MODEL

The numerical simulations were conducted using OpenFOAM 6.0 (CFD Direct 2018). Considering the physics of the siphon and previous numerical studies (Ramajo et al. 2020), the *interFoam* solver was chosen in this study (CFD Direct 2018). This solver uses the volume of fluid (VOF) to capture the air-water interface. A standard k- ε model was applied to resolve the turbulence (Shih et al. 1995), but the details of turbulence modeling are not presented here for brevity. The mesh generation in the present work is done with *snappyHexMesh*, an OpenFOAM meshing utility. The grid independence study has been performed in Zanje et al. (2021) and will not be presented in detail here.

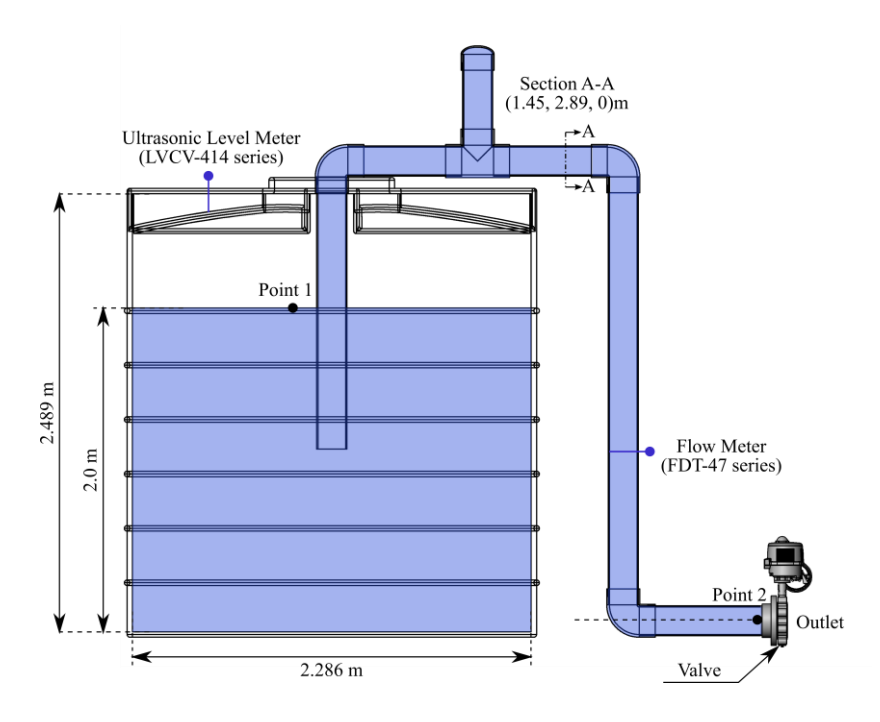


Figure 1: Schematic of experimental siphon facility at the Engineering Center (EC) of the Florida International University, Miami, FL

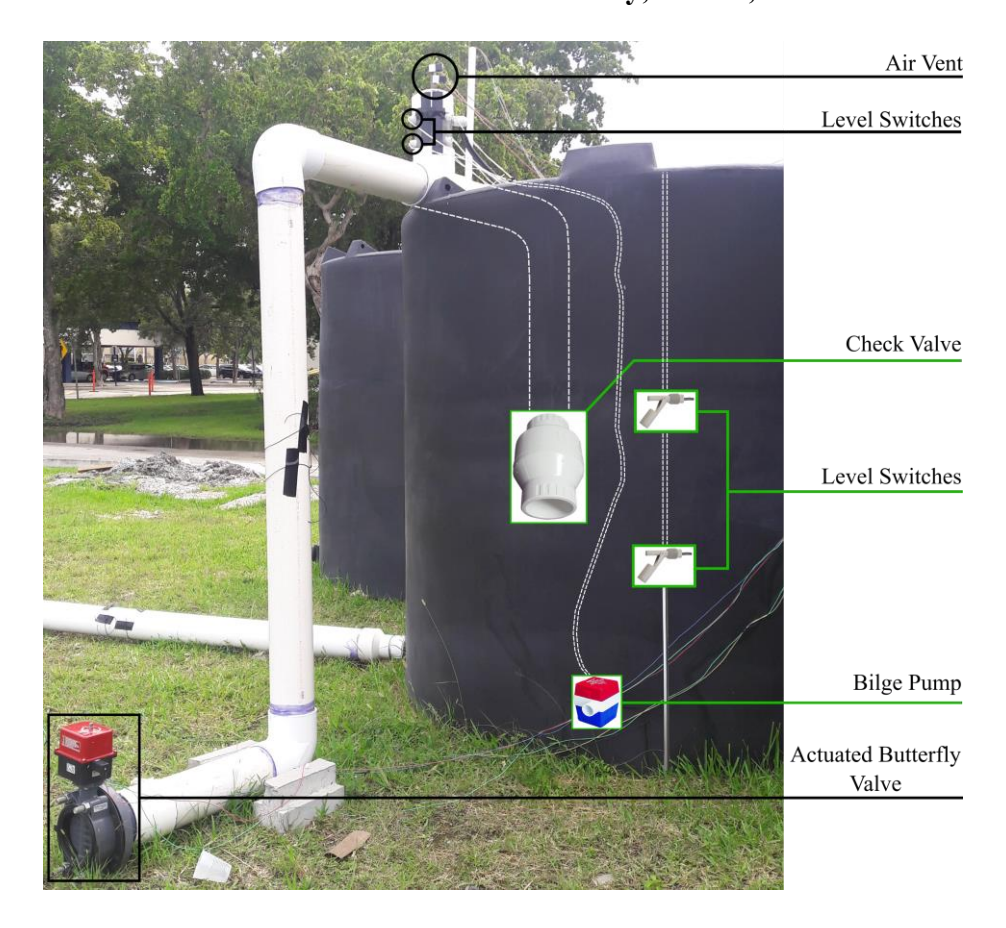


Figure 2. Photo of the experimental siphon facility with primary components

RESULTS

Figure 4 shows the simulated air-water phase fraction data at the center plane for the noleakage condition at eight different times. Figure 5 shows the variation of velocity and pressure at section A-A (shown in Figure 1) with the water level change in the storage tank for the noleakage condition. The water velocity decreases from 2.2 m/s to 1.6 m/s as the water level in the tank drops from 2 m to 1 m. The reduction in water velocity is due to a decrease in induced driving force (Seo et al. 2012). This can also be visualized by the reduction in pressure from 83800 N/m² to 78650 N/m². The siphon flow continues until the water level reaches 1 m in the storage tank. Comparison of CFD, analytical, the energy equation, and the experimental results for water level and discharge time traces are shown in Figure 6. Details on the analytical and energy equation are not presented here for brevity; however the interested reader can find these details in Zanje et al. (2021). As observed in Figure 6, the time trace of water level (blue color lines) and discharge (red color lines) obtained with the CFD model agrees well with the experimental data. The CFD simulations started with water in the tank and pipe at rest and with the downstream valve fully opened, whereas, in the experiments, the actuated butterfly valve was fully opened in about 15 seconds. Thus, the flow in the experiments increased gradually, whereas the flow in the CFD model increased suddenly.

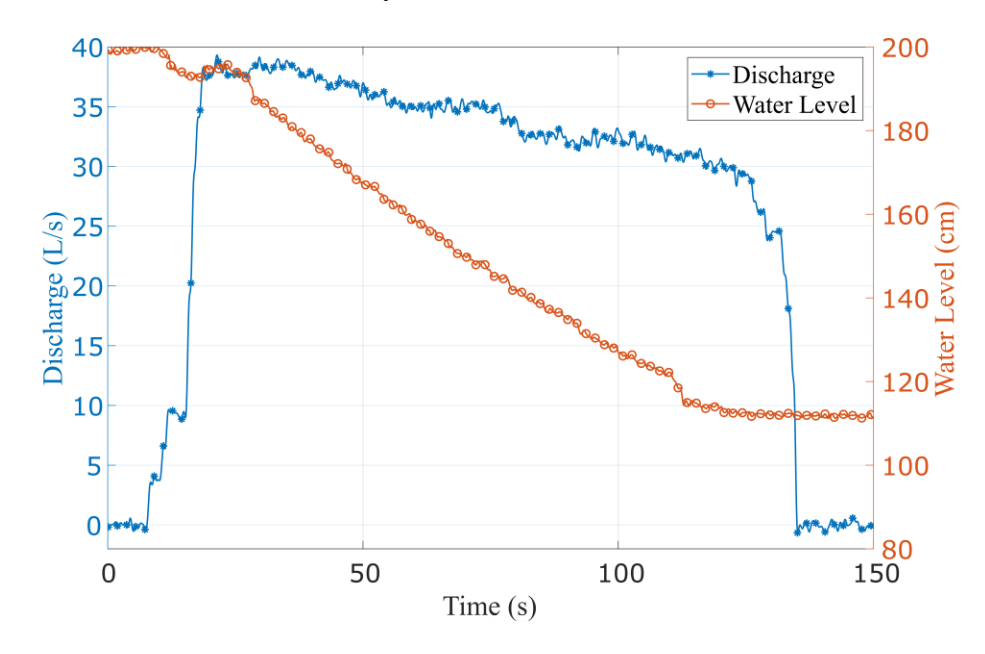


Figure 3. Measured water level and flow discharge traces for the no-leakage case

The impact of pipe leakage on the siphon break phenomena was analyzed for two leaks (e.g., holes) at different positions, one at the top portion of the siphon pipe (case-1) and the second at the lower part of the downhill limb of the siphon pipe (case-2). The positions of the leaks are shown in Figure 7. Figure 8 shows the water velocity and pressure time traces at section A-A for leakage case-1. The leakage is specified at t=20 s. At t=20 s, a sharp rise in the pressure from 82620 N/m² to 97210 N/m² is observed due to ingested air. The water velocity also increased from 2.3 m/s to 2.8 m/s. The water velocity and pressure undergo reduction with successive oscillations until the flow velocity reaches close to zero when the pressure approaches atmospheric pressure.

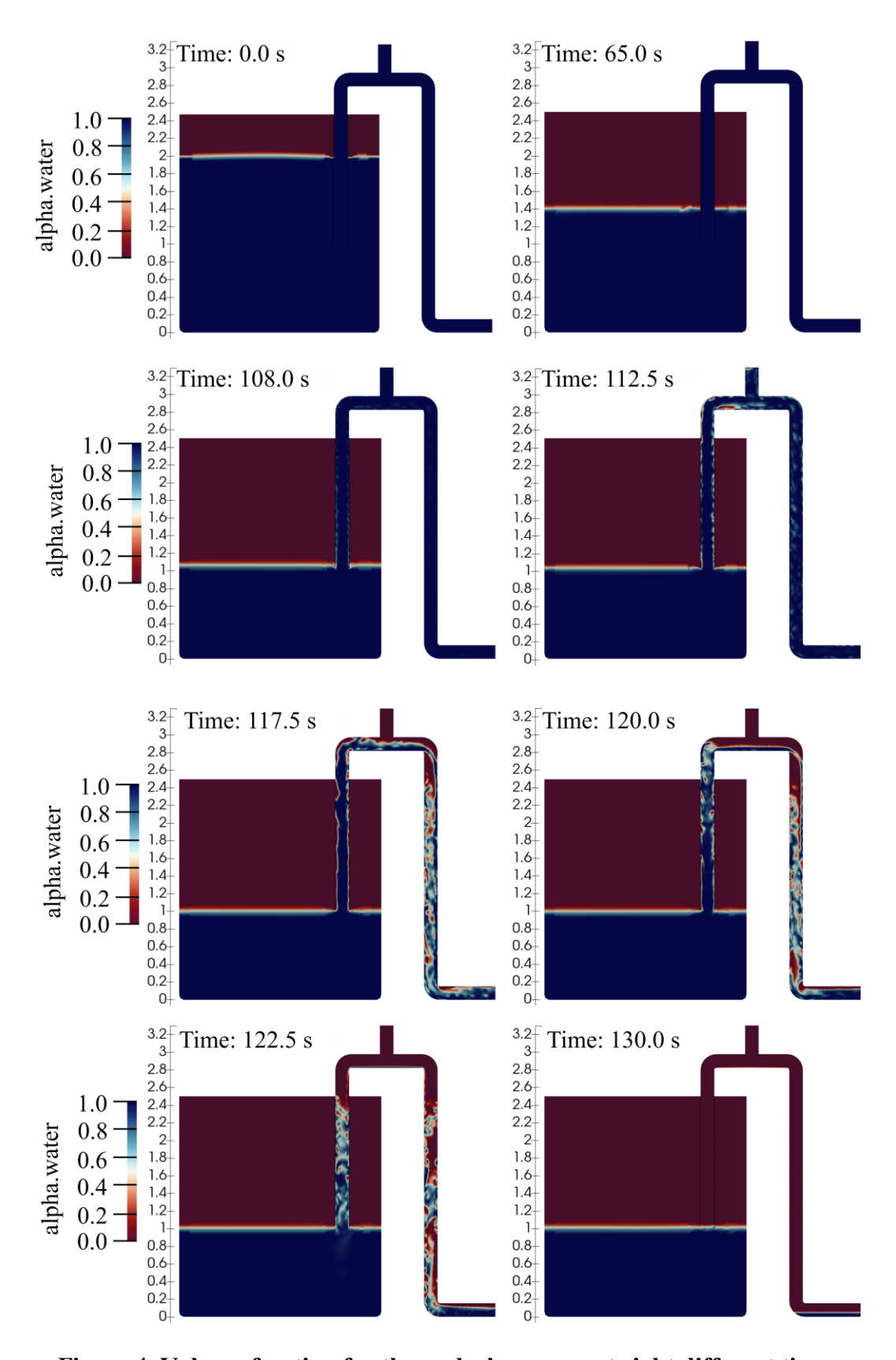


Figure 4. Volume fraction for the no-leakage case at eight different times

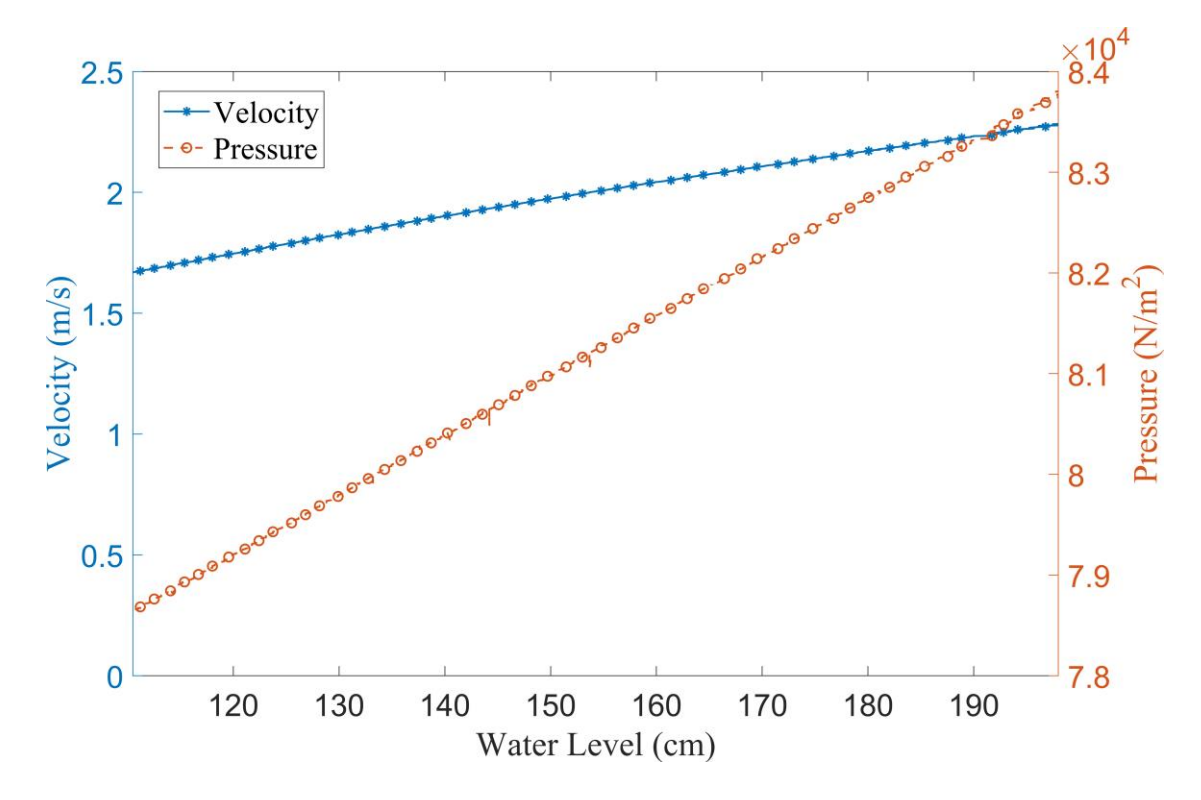


Figure 5. Water velocity and pressure at section A-A in Figure 1 according to the tank water level (no-leakage)

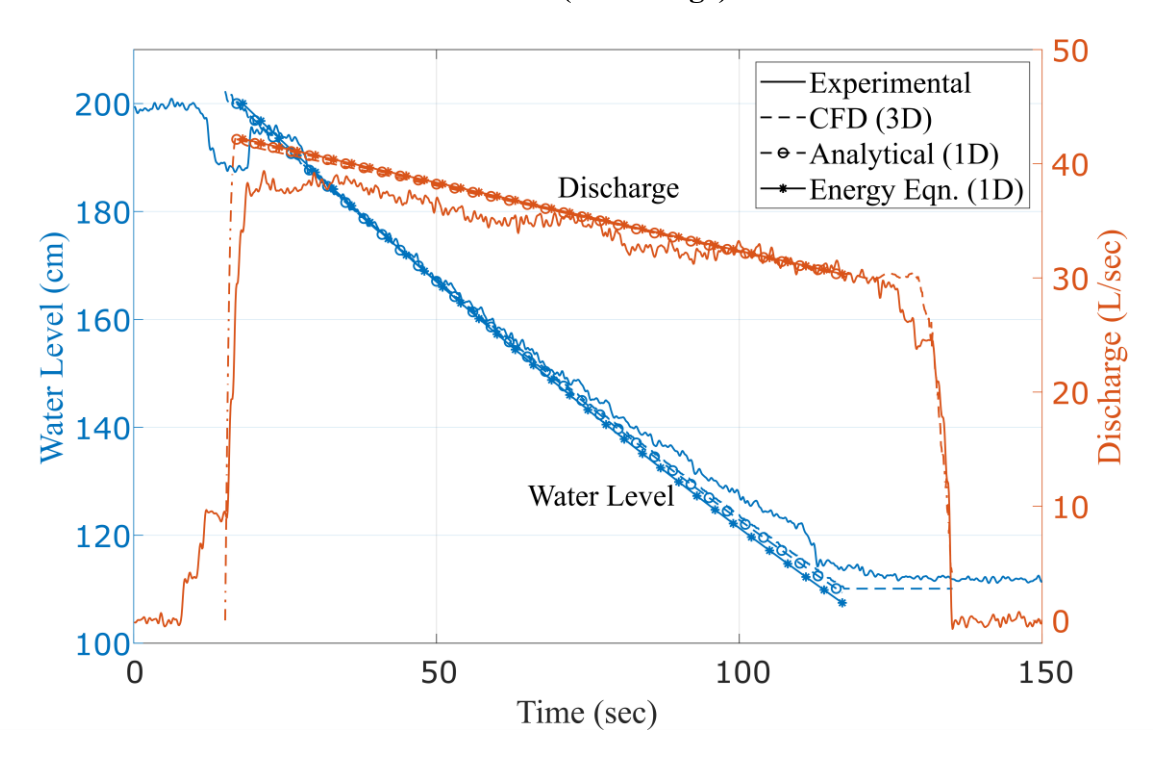


Figure 6. Comparison of numerical, experimental, analytical, and energy equation results for water level (blue color) and discharge (red color)

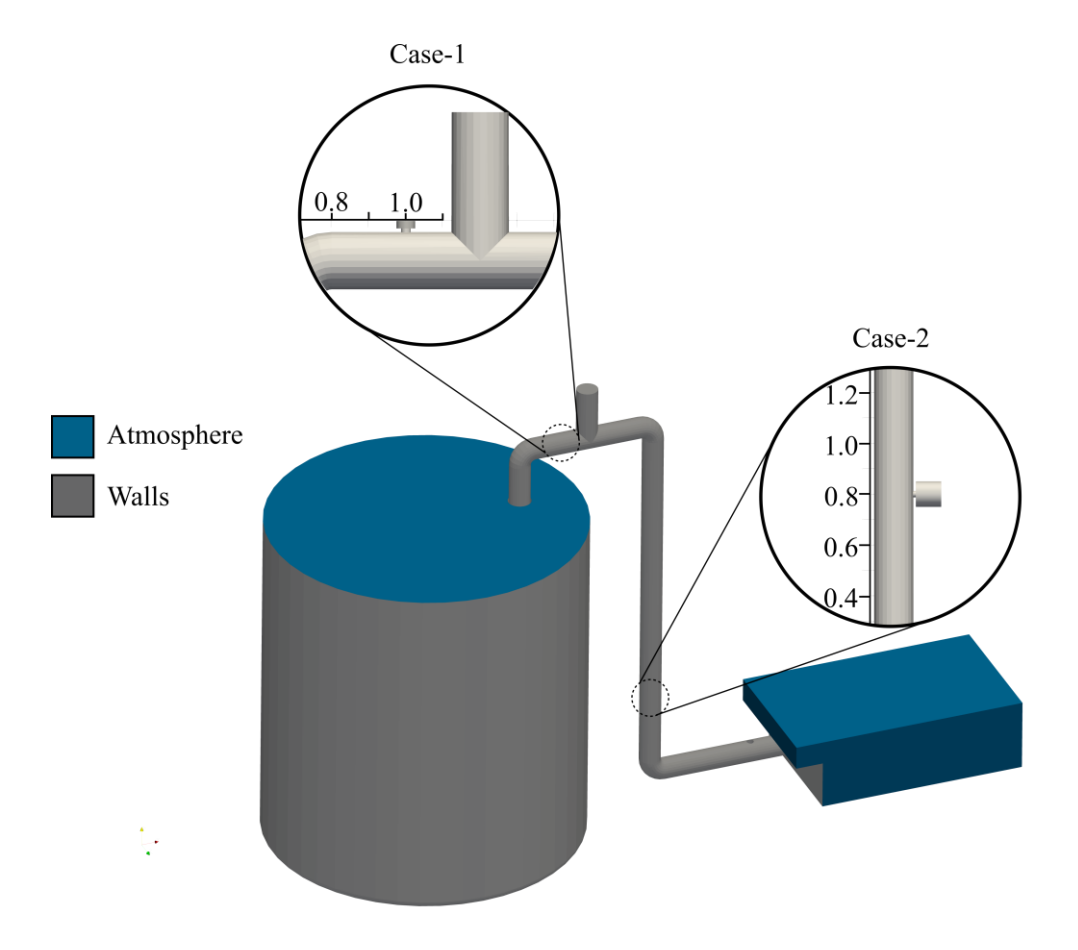


Figure 7. Location of leaks: case-1 and case-2

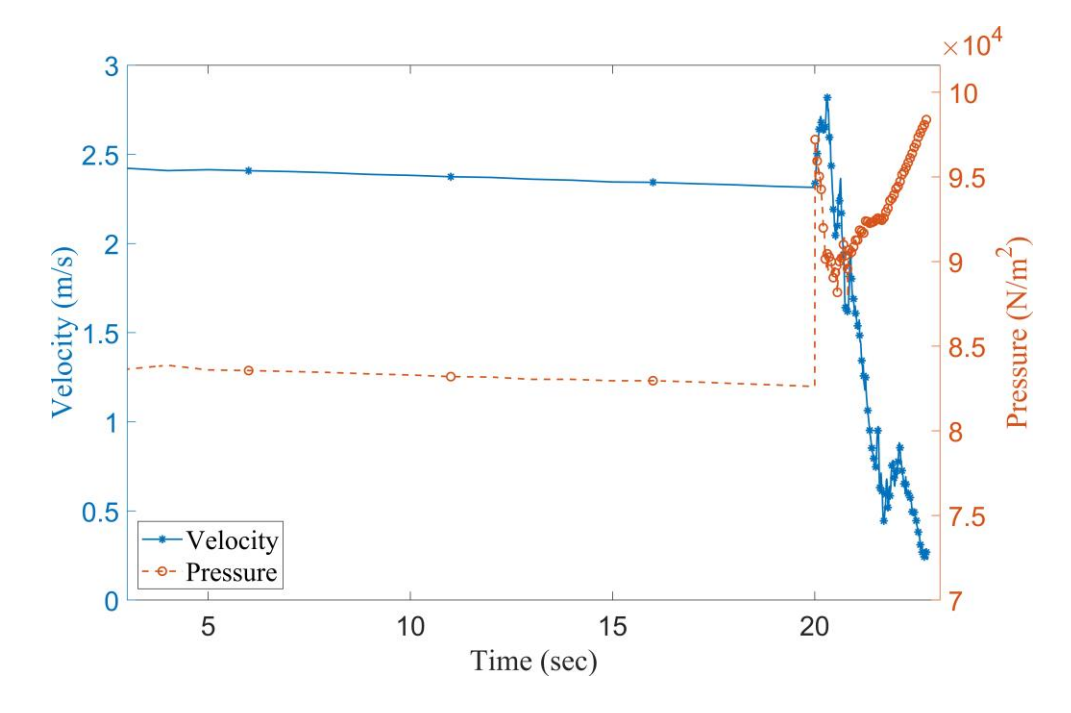


Figure 8. Water velocity and pressure time trace at section A-A for leakage case-1

Figure 9 shows the instantaneous velocity vectors and the air-water phase fraction for leakage case-2 (leak is below the hydraulic grade line). Figure 9b shows that the location and size of the leak ($d_l = D/6$), where d_l is the diameter of the leak hole. From t=0 s to t=44.0 s, the hydraulic grade line is above the leak, causing water to flow from the pipe as the pressure in the pipe is greater than atmospheric pressure. At t=45 s, the hydraulic grade line reaches the leak and starts building the suction pressure. This can be seen in Figure 9c, as the air at atmospheric pressure starts entering the pipe. As time advances and the hydraulic grade line falls, causing an increase in ingested air. Even though air enters the pipe, no siphon break was observed. Figure 9d shows the transport of ingested air at the leak towards the siphon outlet. The inertial force of water in the siphon causes the ingested air to move downstream and avoid the siphon flow break.

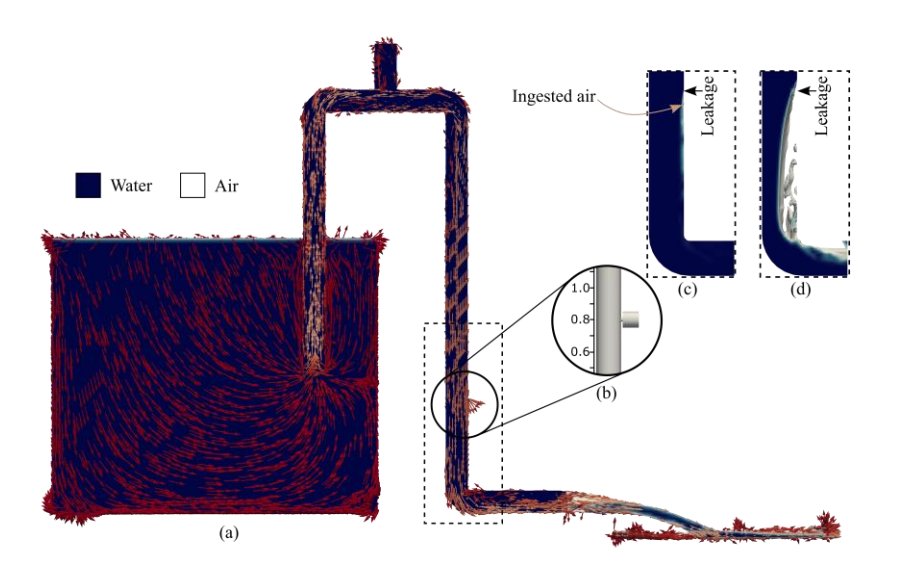


Figure 9. Simulation results for the case-2 (leakage below hydraulic grade line): (a)
Instantaneous velocity vectors, (b) location of leakage, (c) air-water phase fraction at t=45.0 s, (d) air-water phase fraction at t=63.0 s

CONCLUSION

This paper, presents part of the results on Zanje et al. (2021), reports a laboratory and numerical study on siphon flow under no-leakage and leakage conditions. The numerical study has investigated the hydrodynamic characteristics of siphon flows using OpenFOAM. The key results are as follows:

- (1) In general, a good agreement between numerical and experimental results was obtained for the no-leakage condition.
- (2) The position of leakage influenced the flow dynamics. For the leakage at the top horizontal portion of the siphon pipe (case-1), the water undergoes a sudden rise in velocity immediately after the leakage. This leak is above the hydraulic grade line, causing air to ingest in the pipe, leading to siphon breakage.
- (3) As long as the leak is below the hydraulic grade line (case-2), no air is allowed to enter the pipe due to outgoing water flow water from the siphon. Even though the hydraulic grade line falls below the leak, no siphon flow break was observed due to removing ingested air with outgoing water flow. Further studies will evaluate this.

ACKNOWLEDGMENT

This work was supported by the National Science Foundation through NSF/ENG/CBET under Award No. 1805417 and through NSF/DBI/BIO under Award No. 1820778.

REFERENCES

- Aydin, M. C., Öztürk, M., and Yücel, A. (2015). "Experimental and numerical investigation of self-priming siphon side weir on a straight open channel." *Flow Measurement and Instrumentation*, 45, 140–150.
- Babaeyan-Koopaei, K., Valentine, E. M., and Ervine, D. A. (2002). "Case study on the hydraulic performance of Brent Reservoir siphon spillway." *Journal of Hydraulic Engineering*, 128(6), 562–567.
- Bian, L., Verma, V., Rojiali, A., Ozecik, D., and Leon, A. S. (2021). "Operational reliability Assessment of a Remotely Controlled Siphon System for Draining Shallow Storage Ponds" World Environmental and Water Resource Congress 2021, 607–620.
- Cai, L., Yue Sun, H., Quan Shang, Y., and Liang Xiong, X. (2014). "An investigation of flow characteristics in slope siphon drains." *Journal of Zhejiang University SCIENCE A*, 15(1), 22–30.
- CFD Direct. (2018). *OpenFOAM 6.0*. The OpenFOAM Foundation Ltd. London, United Kingdom, https://openfoam.org/.
- Hughes, S. W. (2010). "A practical example of a siphon at work." *Physics Education*, 45(2), 162. Kang, S. H., Ahn, H. S., Kim, J. M., Joo, H. M., Lee, K.-Y., Seo, K., Chi, D. Y., Yoon, J., Jeun, G. D., and Kim, M. H. (2013). "Experimental study of siphon breaking phenomenon in the real-scaled research reactor pool." *Nuclear Engineering and Design*, 255, 28–37.
- Leon, A., and Alnahit, A. (2016). "A remotely controlled siphon system for dynamic water storage management. in *Proc. 6th IAHR Int. Symp. Hydraulic Struct.*, Portland, OR, USA, Jun. 2016, pp. 1–11.
- Leon, A. S., and Verma, V. (2019). "Towards Smart and Green Flood Control: Remote and Optimal Operation of Control Structures in a Network of Storage Systems for Mitigating Floods." In *World Environmental and Water Resources Congress 2019: Watershed Management, Irrigation and Drainage, and Water Resources Planning and Management* (pp. 177-189). Reston, VA: American Society of Civil Engineers.
- Qin, L., Leon, A. S., Bian, L.-L., Dong, L.-L., Verma, V., and Yolcu, A. (2019). "A Remotely-Operated Siphon System for Water Release From Wetlands and Shallow Ponds." in *IEEE Access*, vol. 7, pp. 157680-157687.
- Ramajo, D. E., Corzo, S. F., and Nigro, N. M. (2020). "Numerical Simulation of Siphon Breaker Systems for Open-Type Research Reactors." *Journal of Nuclear Engineering and Radiation Science*, 6(2).
- Ramette, J. J., and Ramette, R. W. (2011). "Siphonic concepts examined: a carbon dioxide gas siphon and siphons in vacuum." *Physics Education*, 46(4), 412.
- Richert, A., and Binder, P. M. (2011). "Siphons, revisited." The Physics Teacher, 49(2), 78–80.
- Seo, K., Kang, S. H., Kim, J. M., Lee, K. Y., Jeong, N., Chi, D. Y., Yoon, J., and Kim, M. H. (2012). Experimental and numerical study for a siphon breaker design of a research reactor. *Annals of Nuclear Energy*, 50, 94-102.

- Shih, T.-H., Liou, W. W., Shabbir, A., Yang, Z., and Zhu, J. (1995). "A new k-ε eddy viscosity model for high reynolds number turbulent flows." *Computers & Amp; fluids*, 24(3), 227–238.
- Verma, V., Bian, L., Ozecik, D., Sirigineedi, S. S., and Leon, A. (2021). "Internet-Enabled Remotely Controlled Architecture to Release Water from Storage Units." *World Environmental and Water Resources Congress* 2021, 586–592.
- Verma, V., Bian, L., Rojali, A., Ozecik, D., and Leon, A. (2020a). "A Remotely Controlled Framework for Gravity-Driven Water Release in Shallow and Not Shallow Storage Ponds." World Environmental and Water Resources Congress 2020, 12–22.
- Verma, V., Vutukuru, K. S., Bian, L., Rojali, A., Ozecik, D., and Leon, A. (2020b). "Reliability and Robustness Evaluation of a Remotely Operated Siphon System for Flood Mitigation during Hurricanes." World Environmental and Water Resources Congress 2020, 31–39.
- Viridi, S., Khotimah, S. N., and Masterika, F. (2011). "Self-Siphon Simulation Using Molecular Dynamics Method." arXiv preprint arXiv:1104.1847.
- Zanje, S. R., Bian, L., Verma, V., Yin, Z., and Leon, A. S. (2021). "Siphon Break Phenomena Associated with Pipe Leakage Location." *Journal of Fluids Engineering*. Submitted for publication.